



# Performance evaluation of membrane-based absorbers employing $\text{H}_2\text{O}/(\text{LiBr} + \text{LiI} + \text{LiNO}_3 + \text{LiCl})$ and $\text{H}_2\text{O}/(\text{LiNO}_3 + \text{KNO}_3 + \text{NaNO}_3)$ as working pairs in absorption cooling systems



Faisal Asfand, Youssef Stiriba, Mahmoud Bourouis\*

Department of Mechanical Engineering – Universitat Rovira i Virgili, Av. Països Catalans No. 26, 43007 Tarragona, Spain

## ARTICLE INFO

### Article history:

Received 20 February 2016

Received in revised form

21 August 2016

Accepted 30 August 2016

Available online 18 September 2016

### Keywords:

Absorption cooling systems

Membrane contactors

CFD simulation

Plate-and-frame membrane absorber

$\text{H}_2\text{O}/(\text{LiBr} + \text{LiI} + \text{LiNO}_3 + \text{LiCl})$

$\text{H}_2\text{O}/(\text{LiNO}_3 + \text{KNO}_3 + \text{NaNO}_3)$

## ABSTRACT

In recent years, rigorous research has been carried out on the use of membrane contactors to design compact absorbers for absorption cooling systems and to extend their use in small scale applications. Moreover, the use of new working fluid mixtures has been suggested for the absorption cooling systems to cope with the limitations and problems associated with the conventional working fluid mixtures. In this study, water/(LiBr + LiI + LiNO<sub>3</sub> + LiCl) with mass compositions in salts of 60.16%, 9.55%, 18.54% and 11.75%, respectively, and water/(LiNO<sub>3</sub> + KNO<sub>3</sub> + NaNO<sub>3</sub>) with mass compositions in salts of 53%, 28% and 19%, respectively, were investigated for air-cooled and multi-stage high temperature absorption cooling systems, respectively. Results show that a 25% increase in the absorption rate can be achieved by using water/(LiBr + LiI + LiNO<sub>3</sub> + LiCl) when compared to water/LiBr at air-cooling thermal conditions. Furthermore, an absorption rate as high as 0.00523 kg/m<sup>2</sup> s is achieved when the water/(LiNO<sub>3</sub> + KNO<sub>3</sub> + NaNO<sub>3</sub>) working fluid mixture is used in the membrane-based absorber of the third stage of a triple effect absorption cooling cycle. In addition, the pressure drop percentage in the case of water/(LiNO<sub>3</sub> + KNO<sub>3</sub> + NaNO<sub>3</sub>) working fluid mixture is significantly lower than the water/LiBr and water/(LiBr + LiI + LiNO<sub>3</sub> + LiCl) working fluid mixtures because of the higher operating pressure.

© 2016 Elsevier Ltd. All rights reserved.

## 1. Introduction

Absorption air-conditioning systems, which can use solar thermal energy, are an interesting alternative for space cooling in summer when compared to vapour compression systems, which use costly mechanical energy input. In summer, the intensity of solar thermal radiation is high and thus an absorption air-conditioning system using solar thermal radiations can better satisfy the cooling demand during the day. Moreover, the refrigerants used in conventional vapour compression air-conditioning systems are not environmental friendly and can contribute to ozone depletion and greenhouse effects, whereas in the absorption air-conditioning systems the working fluid mixtures are environmental friendly. Absorption air-conditioning has been an attractive alternative since the early stages of air-conditioning technologies and continued improvements in the design and configuration of the components of absorption air-conditioning

systems have been suggested and implemented on a commercial scale to improve their performance. The absorber is an important component of an absorption air-conditioning system and as such plays a critical role in the overall performance, size, and capital cost of the system. Both the design and configuration of the absorber significantly influence its performance as heat and mass transfer take place simultaneously in this component. Absorbers used in absorption cooling technology employing water as a refrigerant, operate under static vacuum pressure conditions and are accompanied by a high specific volume of water vapour. This means that the absorber has a direct effect on the size, weight and space requirements of absorption air-conditioning systems. Research is currently being carried out to design more compact absorbers for absorption air-conditioning systems. Recently, research has shown that membrane contactor technology can be used in these systems, especially in the case of the absorber and desorber. The aim is to reduce the size, weight and cost of the system while significantly enhancing the heat and mass transport processes taking place in these components. The use of polymeric hydrophobic microporous membrane contactors in the absorber could also mean a reduction in manufacturing cost. Both numerical and experimental studies

\* Corresponding author.

E-mail address: [mahmoud.bourouis@urv.cat](mailto:mahmoud.bourouis@urv.cat) (M. Bourouis).

## Nomenclature

$c_B$	Boltzmann constant (J/K)
$D$	diffusion coefficient ( $\text{m}^2/\text{s}$ )
$d_p$	membrane pore mean diameter ( $\mu\text{m}$ )
$d_h$	hydraulic diameter (m)
$J$	mass transfer flux ( $\text{kg}/\text{m}^2 \text{ s}$ )
$K$	mass transfer coefficient ( $\text{kg}/\text{m}^2 \text{ s Pa}$ )
$Kn$	Knudsen number, $Kn = \lambda/d_p$
$k$	thermal conductivity (W/m K)
$L$	channel length (m)
$M$	molecular weight (g/mol)
$P$	pressure (Pa)
$p$	vapour pressure of solution (Pa)
$R$	universal gas constant (J/mol K)
$Re$	Reynolds number, $Re = \rho \cdot u \cdot d_h / \mu$
$T$	temperature ( $^{\circ}\text{C}$ , K)
$t$	channel thickness (m)
$X$	LiBr mass fraction

## Greek letters

$\rho$	density ( $\text{kg}/\text{m}^3$ )
$\varepsilon$	porosity
$\delta_m$	membrane thickness ( $\mu\text{m}$ )
$\sigma$	molecular collision diameter (m)
$\tau$	tortuosity
$\lambda$	mean free path (m)
$\mu$	dynamic viscosity ( $\text{kg}/\text{m s}$ )

## Subscripts

$c$	coolant
$H_2O$	water
$int$	solution-membrane interface
$m$	membrane
$s$	solution
$v$	vapour
$w$	wall

## Abbreviations

AMD	Advanced Micro Devices
CFD	Computational Fluid Dynamics

are being carried out to investigate the heat and mass transfer processes in microporous hydrophobic membrane based components. Asfand and Bourouis [1] have extensively reviewed the application of membrane contactors in absorption refrigeration systems. They have reported that the use of microporous membrane contactors in the absorber and desorber of an absorption refrigeration system can, not only enhance the heat and mass transfer performance of the component, but can also allow for a reduction in the size and weight of the component. Thus, introducing polymeric hydrophobic microporous membranes into the design of the absorber and desorber could provide an alternative to achieve highly compact components, which would permit the use of absorption air-conditioning systems in small scale cooling applications, heat-driven automotive air conditioning, and portable cooling. The heat and mass transfer processes can be significantly improved because the microporous membrane contactors provide a wider interfacial area. Microporous membrane contactors in the form of plate-and-frame membrane modules and hollow fiber membrane modules have been investigated to replace the conventional components in absorption refrigeration and air-conditioning systems. The plate-and-frame module is generally selected when water is used as a refrigerant, whereas the hollow fibre module is usually selected for ammonia based absorption systems. The driving force for the refrigerant mass transfer in the case of ammonia/water solution is considered to be the difference in ammonia concentration in the solution and vapour phase whereas in the case of water/LiBr, water vapour partial pressure difference across the membrane is responsible for the refrigerant mass transfer.

Table 1 compares the vapour absorption rates achieved in experimental and numerical studies of plate-and-frame membrane based absorbers employing water/LiBr as a working fluid mixture. In addition to the solution channel thickness, the solution inlet temperature and concentration, the solution mass flow rate at the inlet, the cooling water inlet temperature, and the water vapour pressure are also listed in the table. It is evaluated from the reported data in Table 1 that both the solution channel thickness and the operating conditions significantly affect the absorption performance of the absorber. This is evident from the large discrepancy

in the absorption rate at different conditions. Ali & Schwerdt [2] experimentally analysed a plate-and-frame membrane based absorber and achieved an absorption rate of  $0.00125 \text{ kg}/\text{m}^2 \text{ s}$  at a water vapour pressure of 2.339 kPa, which is more than twice the available pressure in a typical absorber. Ali and Schwerdt [2] reported that their membrane mass transport resistance could have dominated the overall mass transfer process which resulted in poor absorption rates. Numerical simulations performed by Yu et al. [3] show that reducing the solution channel thickness can significantly enhance the absorption rate. They reported that an absorption rate of approximately  $0.0092 \text{ kg}/\text{m}^2 \text{ s}$  is achievable if the solution channel is constrained to a thickness of 0.05 mm. Similarly, Isfahani et al. [4] and Isfahani and Moghaddam [5] experimentally investigated plate-and-frame membrane based absorbers and obtained absorption rates of  $0.00355 \text{ kg}/\text{m}^2 \text{ s}$  and  $0.0060 \text{ kg}/\text{m}^2 \text{ s}$  respectively. In their study, they used solution channel thicknesses of 0.16 mm and 0.10 mm, respectively. It can be concluded from the investigations reported above that the lower absorption rate achieved by Ali and Schwerdt [2] is due to the fact that, in their study, they used solution channel thicknesses of 4.0 mm and 2.0 mm respectively. Furthermore, the experimental studies carried out by Isfahani et al. [4] and Isfahani and Moghaddam [5] suggest that the mass transfer through the solution is the dominant resistance as opposed to the membrane mass transfer resistance. In addition, numerical results reported by Asfand et al. [6] critically evaluated the impact of solution channel thicknesses while investigating the effect of membrane characteristics. They reported that the membrane mass transfer resistance is considerable only when the solution channel thickness is of the order 0.1 mm or lower. It was observed from their results that the membrane characteristics have a less prominent effect on the absorption rate in the case of solution channels with a thickness of the order 0.5 mm or more. They concluded that the solution resistance is the dominant resistance to the refrigerant mass transfer. As opposed to conventional absorbers, the solution film thickness and the velocity can be independently controlled in plate-and-frame membrane absorbers. However, decreasing the solution channel thickness and increasing the solution mass flow rate in order to achieve a higher absorption rate can cause an unacceptable pressure drop along the solution

**Table 1**

Absorption rate achieved during experimental and numerical analyses of plate-and-frame membrane based absorbers employing water/LiBr working fluid mixture.

Reference	Study	Solution channel thickness (mm)	Operating conditions					Absorption rate $\times 10^3$ (kg/m <sup>2</sup> s)
			Solution mass flow rate/Inlet velocity	Solution inlet temperature (°C)	Solution inlet concentration (%)	Vapour pressure (kPa)	Coolant inlet temperature (°C)	
Ali & Schwerdt [2]	Experimental	4.00	8.0 kg/h	27.0	53.55	2.339	NA	1.25
Yu et al. [3]	Numerical	0.05	0.15 m/s	45.0	60.00	0.873	27.0	9.20
Isfahani et al. [4]	Experimental	0.16	0.6 kg/h	25.0	60.00	1.100	25.0	3.55
Isfahani & Moghaddam [5]	Experimental	0.10	0.6 kg/h	25.0	60.00	1.350	25.0	6.00
Asfand et al. [7]	Numerical	0.50	0.005 m/s	35.5	57.82	0.813	25.0	1.00
Bigham et al. [8]	Experimental	0.50	0.05 m/s	32.5	60.00	0.873	27.5	4.00

channel. The higher pressure drop along the solution channel can hinder the performance of the plate-and-frame membrane absorber operating with water as a refrigerant under vacuum conditions. Asfand et al. [7] observed that the pressure drop increases exponentially when the solution channel thickness is reduced. They reported that a 50% decrease in the solution film thickness causes an increase in the accumulative pressure drop by a factor of approximately 7.5, keeping the same solution mass flow rate. They recommended that a solution channel thickness of the order 0.5 mm should be used to avoid higher pressure drops in the solution channel. They numerically investigated the plate-and-frame membrane absorber and achieved an absorption rate of 0.001 kg/m<sup>2</sup> s with a solution channel thickness of 0.5 mm. However, the absorption rate can be enhanced if favourable operating conditions are adopted. It can be seen from Table 1 that a higher absorption rate is achievable if the solution mass flow rate, solution inlet concentration and water vapour pressure difference across the membrane are higher and the solution and coolant inlet temperatures are lower. Bigham et al. [8] experimentally and numerically investigated a plate-and-frame membrane absorber with a solution channel thickness of 0.5 mm and achieved an increase in the absorption rate by a factor of 2.5 from 0.0016 kg/m<sup>2</sup>s to 0.004 kg/m<sup>2</sup>s by the implementation of micro-scale features on the flow channel surface. They reported that the laminar streamlines within the solution film are stretched and folded as a result of the vortices and that the mass transport mode in such a configuration could be changed from a diffusive to an advective mode.

Most of the research in the absorption technology is done using the conventional working fluid mixtures, water/LiBr and ammonia/water with water as a cooling medium. However, many new working fluid mixtures have been proposed and investigated for absorption air-conditioning systems for them to cope with the problems and deficiencies associated with the conventional working fluid mixtures, NH<sub>3</sub>/H<sub>2</sub>O and H<sub>2</sub>O/LiBr and to enhance the performance of the absorber. Moreover, there is a growing interest in air-cooled absorption chillers, for which water/multi-salts mixture is proposed as a working fluid due to its wider range of solubility. However, there is very scarce information in the literature about the absorption process with this non-conventional working fluid. Conventional water/LiBr absorption systems are widely used to supply chilled water for industrial and space cooling applications that require huge cooling capacities. In these systems, cooling towers are used for cooling water to dissipate the heat released in the absorber and condenser. Whereas, the transport sector and the residential sector in which the cooling demand is lower, are currently dominated by vapour compression systems that are run by costly mechanical energy systems. If the heat rejected in the absorber and condenser of an absorption system is directly dissipated to ambient air instead of employing cooling

towers, then it can favour the use of absorption systems in small scale applications. Furthermore, it will not only reduce the investment cost of the installation but also eliminate the maintenance cost of cooling towers. However, the absorber and condenser must operate at higher temperatures to effectively dissipate the heat released into the ambient air and this in turn can increase the risk of crystallization of the solution. Water/LiBr solution has a limited range of solubility which restricts the range of temperatures feasible for air-cooled absorbers and hinders the development of air-cooled absorption systems for cooling applications. Recent research has shown that the addition of other salts to LiBr aqueous solutions can significantly improve their solubility. However, the criteria for selecting an appropriate salt mixture should not only include an increase in the range of solubility but also other aspects of the operation of the machine, such as vapour pressure, viscosity, corrosivity, and thermal and chemical stability. Bourouis et al. [9,10] and Medrano et al. [11] experimentally and numerically investigated an aqueous solution of the quaternary salt system (LiBr + LiI + LiNO<sub>3</sub> + LiCl) with mass compositions in salts of 60.16%, 9.55%, 18.54% and 11.75%, respectively, for air-cooled absorption systems and reported that it is less corrosive and its crystallization temperature is about 35 K lower than that of water/LiBr. The presence of lithium chloride decreases the vapour pressure of the solution. Lithium iodide and lithium nitrate improve the solubility and lithium nitrate reduces corrosion in the system. Thus, the use of a multi-salt mixture can overcome the crystallization problem and allow for the development of air-cooled absorption systems with membrane contactor based components for small scale applications.

Currently, numerical and experimental analyses are being carried out in order to improve the thermal efficiency and increase the COP (coefficient of performance) of absorption cooling systems. Double-effect water/LiBr absorption systems have already been developed for commercial cooling applications. However, the COP achieved in these applications does not reach levels high enough to use the thermal potential of high temperature heat sources efficiently, between 1 and 1.3. In order to make better use of the thermal energy produced by high temperature heat sources and improve the efficiency of absorption cooling systems, the installation of different triple-effect absorption systems has been proposed. The triple-effect absorption cooling cycles are intended, not only to improve the COP, but also to miniaturize the size of the equipment for use in small scale applications. However, the thermal instability, corrosion and crystallization problems of water/LiBr at high temperatures restrict the development of water/LiBr triple-effect cycles for efficient use of thermal energy produced by high temperature heat sources. The conventional water/LiBr working fluid mixture suffers serious problems of corrosion and thermal decomposition at temperatures of over 180 °C.

Davidson and Erickson [12] proposed the use of an aqueous solution of three alkali-metal nitrate salts ( $\text{LiNO}_3 + \text{KNO}_3 + \text{NaNO}_3$ ), called Alkitrane, with mass compositions in salts of 53%, 28% and 19%, respectively, to increase the maximum temperature limit to 260 °C or above for absorption systems. Although the working fluid mixture is compatible with austenitic stainless steel materials at high temperatures, Howe and Erickson [13] reported that this working fluid mixture does not exhibit a wide range of solubility, and consequently its use at low temperatures is limited due to crystallization problems. Therefore, Erickson et al. [14] suggested that Alkitrane can be used in the high temperature components of triple-effect absorption cooling cycles, while the conventional working fluid water/LiBr could be used in the low temperature components. The working fluid Alkitrane is potentially useful when operating at high temperatures in the last stage of a triple-effect cycle because of its non-corrosive nature and high thermal stability up to temperatures of about 260 °C [15]. Moreover, it contains water as a refrigerant, so a membrane based absorber employing microporous hydrophobic membrane contactors can be effective in improving the heat and mass transfer processes and reducing the size of the system.

Experimental and numerical analyses have been carried out to investigate the performance of membrane based absorbers with conventional working fluid mixtures, i.e. water/LiBr and ammonia/water. However, at local levels in the channels, detailed fluid dynamics behaviour and the heat and mass transfer processes of the two non-conventional working fluid mixtures mentioned above needs further investigation. This way the phenomena and the effect of different working fluid mixtures on the heat and mass transfer and flow parameters would be better understood. The purpose of this study is to numerically investigate the use of non-conventional working fluid mixtures in air-cooled and triple-effect absorption cooling systems employing membrane based absorbers. In this work, the CFD code ANSYS/FLUENT 14.0 has been used to perform the simulation of heat and mass transfers in a plate-and-frame membrane absorber. The water/(LiBr + Lil +  $\text{LiNO}_3 + \text{LiCl}$ ) working fluid mixture which is considered as an attractive alternative to water/LiBr in air-cooled absorption cooling systems and the water/( $\text{LiNO}_3 + \text{KNO}_3 + \text{NaNO}_3$ ) working fluid mixture, which can be utilized in the last stage of triple-effect absorption cooling systems, are both numerically investigated. Absorption rate, local temperature and concentration profiles as well as pressure drop along the solution channel are analysed in detail.

## 2. Absorber module

A plate-and-frame membrane absorber has been selected for the analysis in this study. As in the case of absorption cooling system employing water as a refrigerant, the absorber operates under vacuum conditions, so the plate-and-frame membrane module which presents a minimum pressure drop, could be an interesting choice. The structural unit of the absorber configuration with membrane contactors and the sectional view of the absorber are shown in Fig. 1. The configuration of the plate-and-frame absorber is set as such that the solution, coolant and vapour flow in individual flow channels. Each coolant channel serves two solution channels and is fed in a counter flow direction in order to dissipate the heat of absorption from the solution. The first and last cells of the module have half width coolant channels. Similarly, each vapour channel serves two solution channels and can move in a counter flow or co-current flow. The coolant and solution are separated using a metallic plate across which only heat transfer takes place. A microporous hydrophobic membrane sheet is placed at the aqueous solution–water vapour interface in the form of a parallel sheet along the metallic plate. Both heat and mass transfer

processes take place across the membrane sheet. The parallel assembly of the plates and membrane sheets minimizes the pressure drop through the absorber. In this study, a flat sheet membrane contactor made of polypropylene material is considered. Because of the corrosive nature of LiBr solution, Hastelloy C-22 alloy has been used to separate the coolant and solution channels. Hastelloy C-22 has exceptional resistance to a wide variety of chemical process environments. The membrane material characteristics and absorber dimensions are summarized in Table 2.

## 3. Working fluid mixture

The quaternary salt system (LiBr + Lil +  $\text{LiNO}_3 + \text{LiCl}$ ) and the ternary mixture of alkali nitrates ( $\text{LiNO}_3 + \text{KNO}_3 + \text{NaNO}_3$ ) were used as absorbents with water as a refrigerant. Numerical simulations were carried out and the results were compared to those of the conventional working fluid mixture water/LiBr.

### 3.1. Thermophysical properties

In the ANSYS/FLUENT 14.0 code material database water/(LiBr + Lil +  $\text{LiNO}_3 + \text{LiCl}$ ), water/( $\text{LiNO}_3 + \text{KNO}_3 + \text{NaNO}_3$ ) as well as water/LiBr mixture are not available. Therefore, these working fluid mixtures were created in the material panel of the ANSYS/FLUENT 14.0 code and the thermophysical properties of the mixtures were updated in the ANSYS/FLUENT 14.0 code database with user defined functions. Density, viscosity, thermal conductivity, specific heat capacity and diffusion coefficient of the aqueous solutions of the examined working fluid mixtures were estimated as a function of solution concentration and temperature.

#### 3.1.1. Vapour liquid equilibria

The correlation developed by Uemura and Hasaba [16] was used to calculate the vapour pressure of the water/LiBr solution. The vapour pressure data of Koo et al. [17] and the correlation developed by the research group CREVER from Rovira i Virgili University [18] were used to calculate the vapour pressure of the quaternary salt working fluid mixture. To calculate the vapour pressure of the Alkitrane solution, the correlation developed by Álvarez et al. [19] was used.

#### 3.1.2. Density and viscosity

The density and viscosity of the aqueous solution of lithium bromide was calculated using the correlation developed by Lee et al. [20]. The correlation developed by the research group CREVER from Rovira i Virgili University [18] was used to calculate the density and viscosity of the quaternary salt working fluid mixture. To calculate the density and viscosity of the Alkitrane solution, the correlation developed by Álvarez [21] was used.

#### 3.1.3. Specific heat capacity

The correlation reported in Kaita [22] was used to calculate the specific heat capacity of the water/LiBr fluid mixture. The correlations reported in Salavera et al. [23] and Koo et al. [17] were used to calculate the specific heat capacity of the quaternary salt working fluid mixture. The procedure reported by Laliberté [24] was used to calculate the specific heat capacity of the Alkitrane solution.

#### 3.1.4. Thermal conductivity

The thermal conductivity of the water/LiBr fluid mixture was calculated using the correlation of DiGiulio et al. [25]. The correlation developed by the research group CREVER from Rovira i Virgili University [18] was used to calculate the thermal conductivity of the quaternary salt working fluid mixture. To calculate the thermal conductivity of the Alkitrane solution, the method of Aseyev [26]



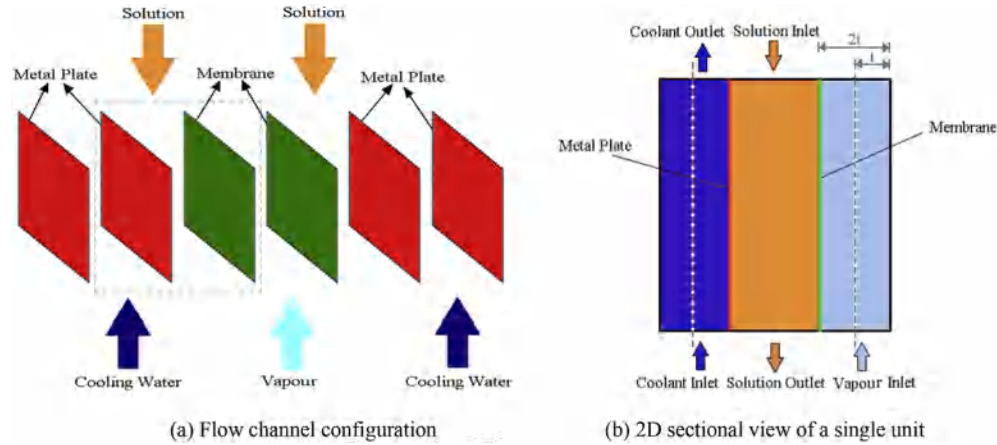


Fig. 1. Plate-and-frame absorber configuration with membrane contactor.

Table 2

Membrane material characteristics and absorber dimensions.

Thickness, $\delta_m$ ( $\mu\text{m}$ )	40
Porosity, $\epsilon$ (%)	85
Tortuosity, $\tau$ ( $\tau = (2 - \epsilon)^2/\epsilon$ )	1.56
Mean pore diameter, $d_p$ ( $\mu\text{m}$ )	1.0
Thermal conductivity, $k_m$ (W/m K)	0.17
Thermal conductivity, $k_w$ (W/m $^\circ$ K)	10
Solution channel thickness, $t$ (mm)	0.5
Solution channel length, $L$ (mm)	200

was used.

### 3.1.5. Enthalpy

The enthalpy of water vapour was calculated using the correlation reported in Florides et al. [27]. The differential enthalpy of dilution was estimated using the procedure reported in Asfand and Bourouis [28]. The specific enthalpy of the aqueous solutions of LiBr, quaternary salt system and Alktrate were calculated using the correlations reported in Refs. [22][18], and [29], respectively.

### 3.1.6. Coefficient of diffusion

The diffusion coefficient of water in the aqueous lithium bromide solution was calculated from the experimental data of Gierow and Jernqvist [30] which was determined at constant temperature and different concentrations. However, at other temperatures the diffusion coefficient was estimated using the equation given below.

$$\frac{D_1\mu_1}{T_1} = \frac{D_2\mu_2}{T_2} \quad (1)$$

where  $D$  is the diffusion coefficient,  $\mu$  is the dynamic viscosity and  $T$  is the temperature. State 1 refers to the values calculated at 25  $^\circ\text{C}$  whereas state 2 refers to the values calculated at any other temperature.

Mass diffusivity coefficient of the Alktrate and quaternary salt working fluid mixtures were estimated using the Stokes-Einstein equation reported in Bird [31]. The method was validated against the known diffusion coefficient of water/LiBr working fluid mixture.

## 4. Numerical model

In this study, CFD numerical simulations were performed in a workstation cluster of 24 AMD Opteron 248 dual core processors

(64 bits) and 7 Intel 3 Ghz processors, with 3 terabytes of disk, linked with a Giga Ethernet in a Linux environment. Simulations were performed in parallel using four processors and each case simulated took approximately 6 days to achieve a steady-state condition. The CFD commercial code ANSYS Fluent 14.0 was used for the numerical simulation which employs a finite volume approach to discretize the governing Navier-Stokes equations into a set of linear equations. The computational domain, boundary conditions and numerical schemes adopted in this study are illustrated in the following subsections.

### 4.1. Model assumptions

The following assumptions are considered in the analytical model for the simulation:

- Steady state conditions.
- Linear coolant temperature rise.
- Vapour channel pressure and temperature are assumed constant.
- Coolant thermophysical properties are assumed constant.
- No heat losses to/or gained from the surroundings of the absorber cells.

### 4.2. Computational domain

A two-dimensional model was developed to simulate the flow, heat and mass transfer processes in a single unit of the plate-and-frame membrane module. To reduce the computational time and reach a converged solution without flow instabilities, the vapour pressure and temperature of the vapour channel were assumed constant. Similarly, a coolant wall temperature function was imposed at the heat transfer plate with a user defined function to incorporate the linearized change in coolant temperature along the channel. The Inlet boundary in the solution flow channel was considered the velocity inlet whereas the outlet boundary condition was specified as the pressure outlet.

The spatial domain of the simplified model was discretized into meshes fine enough to get mesh-independent results based on the independency test. The grids were created in Gambit software and imported into ANSYS Fluent 14.0. Different grid sizes were tested for the 0.5 mm solution channel. The mesh size of  $15 \times 15000$  cells, with a minimum edge size of 0.00002 and a growth factor of 1.2 in the boundary layer, was selected for the simulation analysis. A grid

independence test showed that the maximum error in the absorption rate was less than 1% when the grid size was reduced by a factor of 2.

### 4.3. Governing equation

In the present numerical simulation of heat and mass transfer, the flow in the solution channel is a homogeneous single phase flow. As the species in the solution are well mixed, the relative velocity between the species is negligible. In the absence of relative motion, the governing mass and momentum conservation equations for homogeneous flow are reduced to the single-phase form, therefore, instead of the mixture model, single phase equations are used to perform the simulation with less computational effort. The flow is governed by the Navier-Stokes equations. The continuity, momentum, energy and specie transport equations are solved to perform steady-state heat and mass transfer analyses. These equations are given in the ANSYS/FLUENT 14.0 theory guide.

The driving force for the refrigerant vapour mass transfer across the membrane in a water-LiBr absorber is the difference in vapour pressure and partial pressure of water vapour in the aqueous solution. The mass transfer flux across the membrane is given by Martinez and Rodriguez-Maroto [32] as follows:

$$J = K_m(P_v - p_{int}) \quad (2)$$

where  $J$  is the mass transfer flux of water vapour absorbed in the solution,  $P_v$  is the water vapour pressure and  $p_{int}$  is the equilibrium water vapour partial pressure of the solution at the solution-membrane interface.  $K_m$  is the membrane equivalent mass transfer coefficient.

Mass transport through a microporous membrane can take place by different mechanisms depending on the flow regime. Thus, it is important to determine the flow regime in order to accurately calculate the mass flux through the membrane. Flow through a porous membrane can be classified into viscous, transitional, or free molecular flow regimes, depending on the magnitude of the Knudsen (Kn) number. The Kn number is defined as the ratio of the mean free path ( $\lambda$ ) to the pore diameter ( $d_p$ ):

$$Kn = \lambda/d_p \quad (3)$$

where  $\lambda$  is the mean free path and is calculated as:

$$\lambda = \frac{c_B \cdot T}{\sqrt{2} \cdot \pi \cdot \sigma^2 P} \quad (4)$$

where  $c_B$  is the Boltzmann constant ( $1.38 \times 10^{-23}$  J/K),  $\sigma$  is the molecular collision diameter ( $2.7 \times 10^{-10}$  m for water vapour),  $T$  is the absolute temperature in K and  $P$  is mean total pressure within the membrane pore in Pa.

For  $Kn > 10$ , collision between molecules and pore walls is dominant, the gas transport takes place in the free molecular regime and the flow is known as Knudsen flow. When  $Kn < 0.01$ , collisions between gas molecules dominate and viscous flow occurs which results in rapid convective transport. A transitional flow regime exists if  $0.01 < Kn < 10$  and according to the Dusty-Gas model, the mass transfer through a membrane consists of both diffusion and viscous fluxes.

In this study, the mean membrane pore diameter is 1  $\mu\text{m}$  and at vapour pressure of 1.3 kPa and 30 kPa, the mean free path of water molecules is 9.8  $\mu\text{m}$  and 0.5  $\mu\text{m}$ , respectively, therefore the Knudsen number value lays in the transitional flow regime for both cases and the vapour transport through the microporous membrane pores takes place via both the diffusion and convective transport

mechanisms. The membrane mass transfer coefficient in the transitional flow regime can be calculated as:

$$K_m = \frac{M_{H_2O}}{\delta_m} \left( \frac{D_k}{RT_m} + \frac{P_m B_0}{RT_m \mu_v} \right) \quad (5)$$

where  $M_{H_2O}$  is the molecular weight of water,  $\delta_m$  is the membrane thickness,  $R$  is the universal gas constant and  $T_m$  is the mean membrane temperature which is calculated as the average of vapour and solution interface temperatures.  $D_k$  is the Knudsen diffusion coefficient and for porous solid it can be calculated as:

$$D_k = \frac{\varepsilon d_p}{3\tau} \left( \frac{8RT_m}{\pi M_{H_2O}} \right)^{\frac{1}{2}} \quad (6)$$

where,  $\varepsilon$  is the membrane porosity,  $\tau$  is the tortuosity of the membrane and  $d_p$  is the mean membrane pore diameter.

$$B_0 = \frac{\varepsilon d_p^2}{32\tau} \quad (7)$$

where,  $\mu$  is the viscosity and  $P$  is the pressure.

The mass transfer flux, which is the vapour mass that is absorbed in the solution, is added as a mass source term in the continuity equation and a specie source term in the species transport equation. A user defined function is implemented at the solution-membrane interface to model the vapour mass transfer across the membrane. Similarly, with a user defined function at the solution-membrane interface, the heat of absorption in the solution is added to the energy equation as a source term. The heat of absorption is expressed as the change in the enthalpy of water as it undergoes a phase change from vapour to liquid phase plus the differential heat of dilution of the absorbent.

### 4.4. Numerical scheme

The governing equations of continuity, diffusion and energy are used to perform a numerical analysis of coupled heat and mass transfer processes in a plate-and-frame membrane absorber. As the solution flow Reynolds number is low, a laminar model is selected for the analysis. The calculations were performed by a combination of the PISO (Pressure-Implicit with Splitting of Operators) pressure-velocity coupling scheme, part of the SIMPLE family of algorithms, and the first-order accurate implicit scheme for the linearized discretized equations in the segregated solver [33,34]. The Second-order upwind discretization scheme is used to compute advection terms. For the energy and species equations, the second-order discretization scheme was used. In the present work, the numerical computation is considered to have converged when the scaled residuals of the different variables are lowered by tenth orders of magnitude and the steady state results are analysed.

## 5. Results and discussion

CFD simulations are capable of predicting the detailed behaviour of heat and mass transfer phenomena at local regions, thus, a clear pattern of the temperature and concentration gradients and the velocity profiles are obtained.

The current CFD numerical model was validated in a previous study [7] by comparing the local absorption rates predicted along the length of the channel with the numerical results reported by Yu et al. [3]. These authors considered water/LiBr as a working pair and a solution channel of 0.05 mm thickness and 20 mm long. A solution inlet velocity of 0.0182 m/s, and an inlet solution concentration and temperature of 60% and 55 °C, respectively, were considered in

their study. A linear temperature profile was considered along the coolant wall. The local absorption rates predicted by the CFD model were compared with the local absorption rates obtained by Yu et al. [3] at the same operating conditions. The CFD results showed close agreement with the literature data producing a mean absolute percentage error of 4.82%.

In this section, an analysis is carried out to study in detail the absorption performance of a water/(LiBr + Lil + LiNO<sub>3</sub>+°LiCl) working fluid mixture with mass compositions in salts of 60.16%, 9.55%, 18.54% and 11.75%, respectively, at thermal operating conditions of an air-cooled absorption cooling system and compare the results with those of a water/LiBr solution. In addition, a parametric study is performed to investigate in detail the performance of a water/(LiNO<sub>3</sub>+°KNO<sub>3</sub>+°NaNO<sub>3</sub>) working fluid mixture with mass compositions in salts of 53%, 28% and 19%, respectively, at the operating conditions of the last stage of a triple-effect absorption cooling system. It is worth noting that the selected operating conditions at which the simulations are carried out in this study lie in the regime where the solutions are not prone to crystallization problem.

Fig. 2 shows the results of the analysis carried out to investigate the performance of a membrane-based absorber at air-cooling thermal conditions employing water/(LiBr + Lil + LiNO<sub>3</sub>+LiCl) and water/LiBr working fluid mixtures. Solution Reynolds number and other input variables were kept constant. The input variables for the analysis correspond to the operating conditions considered in the experimental analysis performed by Bourouis et al. [9,10] given in Table 3. It can be seen that a higher absorption rate is achieved in the case of water/(LiBr + Lil + LiNO<sub>3</sub>+LiCl) with a 64.2% inlet solution concentration when compared to water/LiBr with a 60% inlet solution concentration. However, the water/(LiBr + Lil + LiNO<sub>3</sub>+LiCl) working fluid mixture with a 61% inlet solution concentration yields a lower absorption rate. It is evaluated that a water/(LiBr + Lil + LiNO<sub>3</sub>+LiCl) working fluid mixture is more advantageous at higher solution concentrations and this makes it a better choice for air-cooled absorption cooling systems. In contrast, water/LiBr cannot operate at higher concentrations due to the crystallization problem. It is noted that a higher absorption rate is achieved at the inlet of the absorber due to the low mass fraction of water in the solution at the inlet and a lower solution interface temperature. A tendency for the absorption rate to decrease is observed in the first quarter of the absorber whereas almost a steady absorption rate is achieved in the latter part of the absorber. Initially, a high mass transfer flux is observed as the

**Table 3**

Input conditions for the CFD analysis of water/LiBr and water/(LiBr + Lil + LiNO<sub>3</sub>+°LiCl) working fluid mixtures.

Parameter	Base value
Absorber pressure, Pa	1.3 kPa
Inlet solution temperature, T <sub>s</sub>	45 °C
Inlet solution concentration, X <sub>s</sub>	60, 61, 64.2%
Solution Reynolds Number, Re	2
Cooling wall temperature, T <sub>c</sub>	35–43 °C

solution concentration in the absorbent is high, however, the absorption rate decreases sharply as concentration and temperature boundary layers are developed consequently forming a resistance to the absorption of refrigerant molecules into the solution. A steady mass transfer occurs in the latter part of the channel as in addition to the refrigerant molecules diffusion into the bulk solution, the coolant wall linearly dissipates the heat of absorption and allows the solution to cool down and maintain the absorption capacity of the solution. It is observed that a 25% increase in the overall absorption rate can be achieved by using a water/(LiBr + Lil + LiNO<sub>3</sub>+LiCl) working fluid mixture with a 64.2% inlet solution concentration. In addition, the absorption rate is higher by a factor of 1.67 when the solution inlet concentration of 64.2% is used instead of the 61% concentration in the case of the water/(LiBr + Lil + LiNO<sub>3</sub>+°LiCl) working fluid mixture.

The bulk solution temperature, coolant temperature and the solution-membrane interface temperature are graphically represented along the channel length in Fig. 3. The bulk solution temperature decreases from 318.15 K to 310.30 K, 309.94 K and 310.80 K in the case of water/LiBr, water/(LiBr + Lil + LiNO<sub>3</sub>+°LiCl) with a solution inlet concentration of 61% and water-(LiBr + Lil + LiNO<sub>3</sub> + LiCl) with a solution inlet concentration of

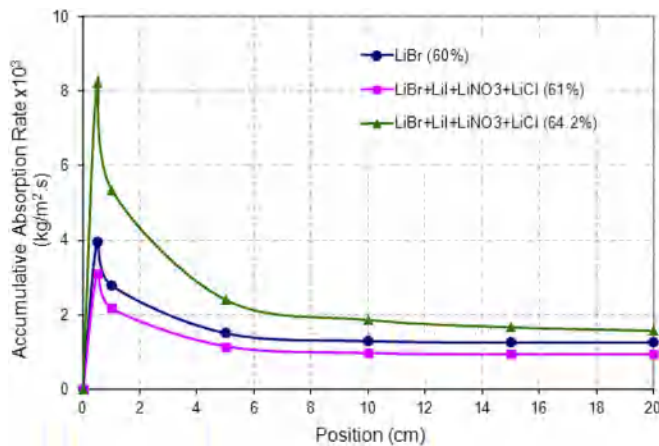


**Fig. 2.** Comparison of accumulative absorption rate of the working fluid mixtures along the channel length.

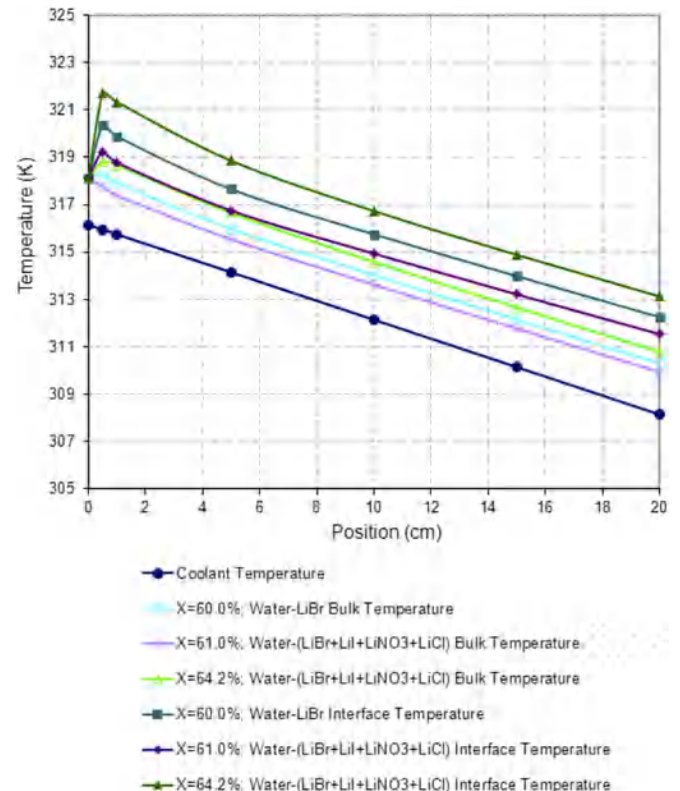


**Fig. 3.** Temperature profiles of the working fluid mixtures along the channel length.



64.2%, respectively. It can be seen that the solution-membrane interface temperature is higher than the bulk solution temperature for all the working fluid mixtures. This is because of the heat of absorption which is generated at the solution-membrane interface. A sharp increase in the interface temperature is observed initially because of the higher absorption rate achieved at first as a result of the higher concentration of the absorbent. The solution-membrane interface temperature decreases from 320.39 K, 319.25 K and 321.69 K–312.26 K, 311.54 K and 313.13 K in the case of water/LiBr, water/(LiBr + LiI + LiNO<sub>3</sub>+°LiCl) with a solution inlet concentration of 61% and water/(LiBr + LiI + LiNO<sub>3</sub>+°LiCl) with a solution inlet concentration of 64.2%, respectively. It was observed that both the bulk solution and the solution membrane interface temperature of the water/(LiBr + LiI + LiNO<sub>3</sub>+°LiCl) working fluid mixture with a solution inlet concentration of 64.2% was higher than that of the water/LiBr solution because the higher absorption rate leads to generation of higher heat of absorption.

Fig. 4 shows the bulk solution concentration and the solution-membrane interface concentration along the channel length. The mass fraction of the absorbent in the bulk solution decreases along the channel length due to the absorption of refrigerant molecules into the solution. It is observed that both the bulk solution concentration and the interfacial solution concentration decrease at the same rate thus producing a transverse concentration gradient along the solution channel to the end. As the concentration difference between the bulk solution and the solution-membrane interface also acts as a driving force for the mass transfer, water vapour absorption is observed up to the channel exit. It is worth noting that the mass fraction of water in the bulk solution and at the solution-membrane interface increases along the channel length, however, both the bulk solution temperature and the solution-membrane interface temperature decrease along the channel length. This causes a decrease in the partial pressure of the

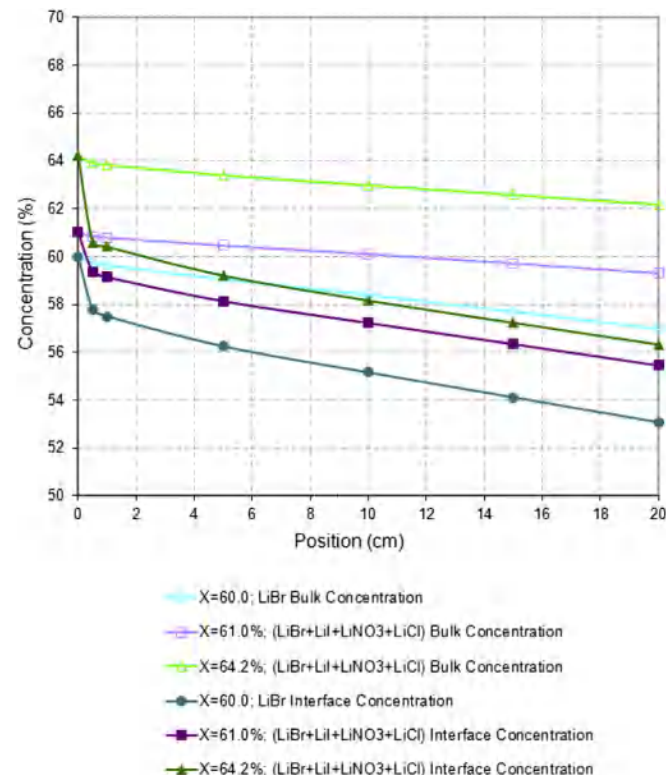


Fig. 4. Concentration profiles of the working fluid mixtures along the channel length.

water vapour in the solution and an increase in the absorption capacity.

Fig. 5 shows the accumulative absorption rate achieved considering the water/(LiNO<sub>3</sub>+°KNO<sub>3</sub>+°NaNO<sub>3</sub>) working fluid mixture at different solution flow Reynolds numbers. The solution flow Reynolds number was increased from 1 to 8 while all other input parameters were kept constant in the simulation. The input variables for the analysis correspond to the operating conditions considered in the experimental analysis performed by Álvarez [21] given in Table 4. It can be seen that the absorption rate increases with an increase in the inlet velocity of the solution. Initially a high mass transfer flux is observed as the solution concentration is high, however, the absorption rate decreases sharply as concentration and temperature boundary layers are developed and resist the absorption of refrigerant molecules into the solution. A steady mass transfer occurs in the latter part of the channel as the coolant wall linearly dissipates the heat of absorption and allows the solution to cool down which increase the absorption capacity of the solution. Initially, the increase in the overall absorption rate is more significant below the solution flow Reynolds number of 2, whereas a linear increase in the absorption rate is achieved when the solution flow Reynolds number is increased from 2 to 8. The increase in the solution velocity brings fresh layers of solution near the membrane interface and increases the absorption capacity, however further-increasing the solution velocity decreases the solution residence time and minimizes the diffusion of water vapours across the solution causing a negative effect on the absorption mass flux. Consequently, the increase in the absorption rate is not very significant when the solution mass flow rate is increased at very high solution flow Reynolds numbers. The absorption rate was increased by a factor of 2 when the solution flow Reynolds number was increased from 1 to 8.

Figs. 6 and 7 show the contours of temperature and the concentration profiles at local levels in the case of water/(LiNO<sub>3</sub>+°KNO<sub>3</sub>+°NaNO<sub>3</sub>) working fluid mixture. Due to the higher aspect ratio of the channel, only the inlet, exit and the middle part of the channel are shown for the 0.5 mm solution channel. Fig. 6 depicts temperature values at local regions from which it can be observed that a temperature gradient exists across the width of the channel. It can be seen that the temperature near the solution-membrane interface (right side) is higher than the bulk solution temperature. This is because of the heat of absorption which is generated at the solution-membrane-interface. The temperature gradient in the transverse direction is higher in the case of higher Reynolds

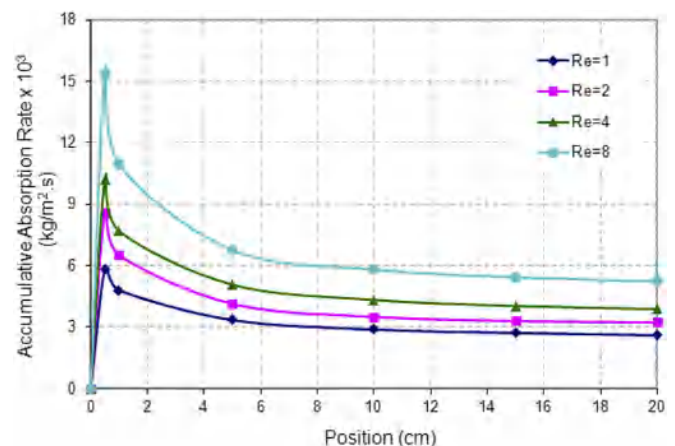
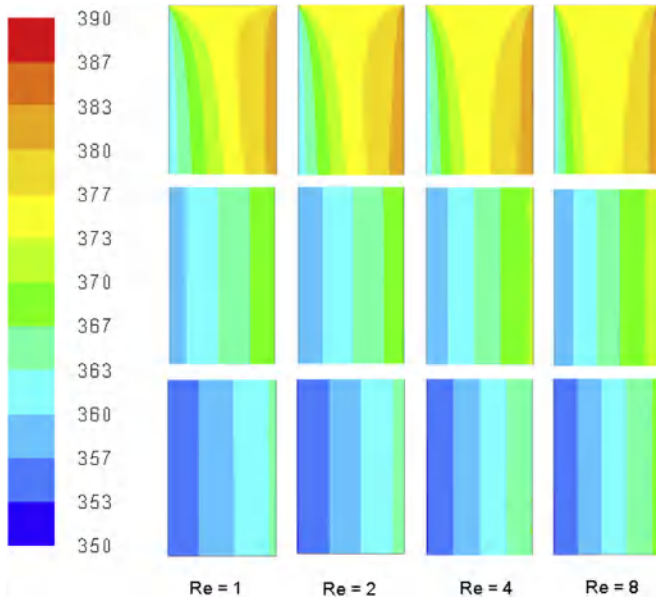


Fig. 5. Accumulative absorption rate along the channel length at different solution Reynolds number.



**Table 4**  
Input conditions for the CFD analysis of water/(LiNO<sub>3</sub> + KNO<sub>3</sub> + NaNO<sub>3</sub>) working fluid mixture.

Parameter	Base value
Absorber pressure, Pa	30 kPa
Inlet solution temperature, T <sub>s</sub>	93 °C
Inlet solution concentration, X <sub>s</sub>	82%
Solution Reynolds Number, Re	1–8
Cooling wall temperature, T <sub>c</sub>	80–88 °C



**Fig. 6.** Contours of temperature profile at different solution Reynolds numbers in the case of water/(LiNO<sub>3</sub> + KNO<sub>3</sub> + NaNO<sub>3</sub>) working fluid mixture.

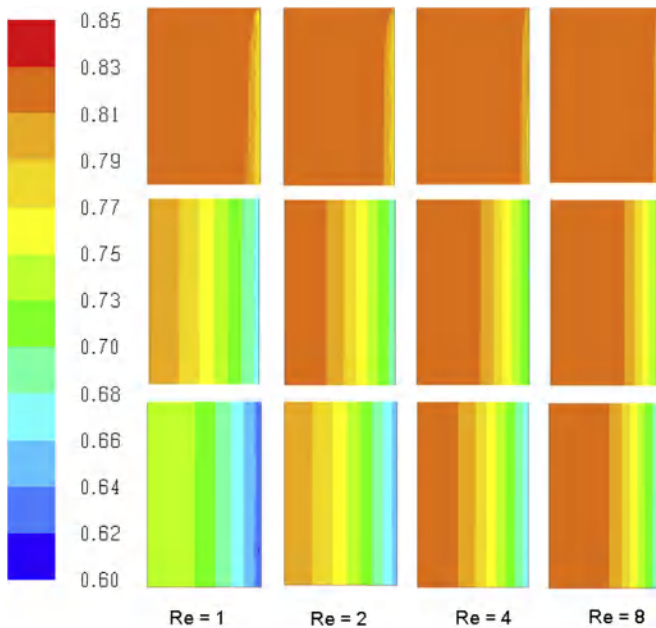


**Fig. 7.** Contours of concentration profile at different solution Reynolds numbers in the case of water/(LiNO<sub>3</sub> + KNO<sub>3</sub> + NaNO<sub>3</sub>) working fluid mixture.

number because of the higher absorption rate which leads to the generation of higher heat of absorption. In addition, the

temperature difference between the bulk solution and the solution-membrane interface is higher near the inlet of the channel and then decreases downwards by about 6 K. This is because of the higher absorption rate at the inlet which generates more heat at the solution-membrane interface and thus a higher temperature gradient is observed. Fig. 7 shows the solution concentration at a local level. It can be seen that the absorbent concentration in the solution is lower at the solution-membrane interface (right side) due to the absorption of refrigerant molecules at the interface. The refrigerant molecules diffuse across the solution at a low rate due to the low diffusivity which gives rise to a concentration gradient across the solution channel. The concentration boundary layer developed at the solution-membrane interface also plays an important role in limiting the mass transfer rate across the membrane. The concentration boundary layer decreases when the solution flow Reynolds number is increased. This occurs as the increase in the solution velocity brings fresh layers of solution with higher absorbent concentration near the membrane interface which increases the absorption capacity.

Fig. 8 shows the overall pressure drop percentage along the solution channel for the three working pairs, namely water/(LiNO<sub>3</sub> + KNO<sub>3</sub> + NaNO<sub>3</sub>), water/LiBr and water/(LiBr + LiI + LiNO<sub>3</sub> + LiCl). The solution pressure at the absorber exit is set as the absorber operating pressure which is 1.3 kPa in the case of water/LiBr and water/(LiBr + LiI + LiNO<sub>3</sub> + LiCl) and 30 kPa in the case of water/(LiNO<sub>3</sub> + KNO<sub>3</sub> + NaNO<sub>3</sub>). The overall pressure drop percentage is calculated with reference to absorber inlet pressure. It can be seen that the overall pressure drop percentage is higher in the case of the water/(LiBr + LiI + LiNO<sub>3</sub> + LiCl) working fluid mixture as opposed to the water/LiBr solution. This is because of the higher viscosity of water/(LiBr + LiI + LiNO<sub>3</sub> + LiCl). Despite the higher viscosity of the Alkitrade solution, the pressure drop percentage is lower compared to water/LiBr and water/(LiBr + LiI + LiNO<sub>3</sub> + LiCl) working fluid mixtures because of the higher operating pressure of the absorber. It means that in case of water/(LiNO<sub>3</sub> + KNO<sub>3</sub> + NaNO<sub>3</sub>), higher solution mass flow rate can be used to achieve a higher absorption rate without affecting the performance of the absorber. The pressure drop percentage of water/(LiBr + LiI + LiNO<sub>3</sub> + LiCl) with a 64.2% solution inlet concentration is about 9 times higher compared to that of a water/(LiNO<sub>3</sub> + KNO<sub>3</sub> + NaNO<sub>3</sub>) working fluid mixture.

**6. Conclusion**

In this study, a detailed analysis of a membrane based absorber has been performed to investigate the heat and mass transfer

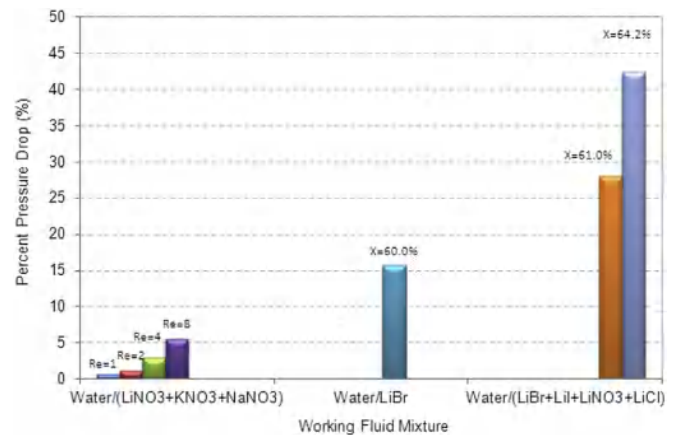


**Fig. 8.** Comparison of percent pressure drop along the solution channel length.

processes at local levels in the flow channels using CFD approach. Introducing polymeric hydrophobic microporous membranes into the absorber design can be one of the alternatives for achieving highly compact absorbers with enhanced heat and mass transfer processes. Working fluid mixtures, water/(LiBr + LiI + LiNO<sub>3</sub>°+°LiCl) with mass compositions in salts of 60.16%, 9.55%, 18.54% and 11.75%, respectively, and water/(LiNO<sub>3</sub>°+°KNO<sub>3</sub>°+°NaNO<sub>3</sub>) with mass compositions in salts of 53%, 28% and 19%, respectively, were investigated for air cooled and multi-stage high temperature heat source absorption cooling systems, respectively. These non-conventional working fluid mixtures are able to cope with the limitations of the conventional water/LiBr working pair. Water/LiBr fluid mixture is prone to crystallization at air-cooling thermal conditions. In addition, it cannot operate in the last stage of a triple-effect absorption cooling system driven by high temperature heat sources (>200 °C) because of thermal instability, crystallization and corrosion problems.

The simulation results provide a deep insight into the heat and mass transfer processes in membrane based absorbers. The results of the CFD simulations are useful and play an important role in the design of membrane based absorbers using non-conventional working fluid mixtures. Results show that a 25% increase in the absorption rate can be achieved by using water/(LiBr + LiI + LiNO<sub>3</sub>°+°LiCl) rather than water/LiBr at air cooling thermal conditions. Furthermore, an absorption rate as high as 0.00523 kg/m<sup>2</sup> s is achieved when a water/(LiNO<sub>3</sub>°+°KNO<sub>3</sub>°+°NaNO<sub>3</sub>) working fluid mixture is used in the membrane-based absorber of the third stage of a triple-effect absorption cooling cycle. In addition, the pressure drop percentage in the case of the water/(LiNO<sub>3</sub>°+°KNO<sub>3</sub>°+°NaNO<sub>3</sub>) working fluid mixture is significantly lower than that of the water/LiBr and water/(LiBr + LiI + LiNO<sub>3</sub>°+°LiCl) working fluid mixtures because of the higher operating pressure.

## Acknowledgements

This study is part of an R&D project funded by the Spanish Ministry of Economy and Competitiveness (DPI2012-38841-C02-02). The authors gratefully acknowledge the Spanish Ministry of Economy and Competitiveness (CTQ2013-46799-C2-1-P) for funding the ANSYS/FLUENT licence. Faisal Asfand gratefully acknowledges the Rovira i Virgili University for granting the Martí-Franquès research fellowship 2012 (2012BPURV-50) to pursue a doctorate degree.

## References

- [1] Asfand F, Bourouis M. A review of membrane contactors applied in absorption refrigeration systems. *Renew Sustain Energy Rev* 2015;45:173–91.
- [2] Ali AHH, Schwerdt P. Characteristics of the membrane utilized in a compact absorber for lithium bromide–water absorption chillers. *Int J Refrig* 2009;32:1886–96.
- [3] Yu D, Chung J, Moghaddam S. Parametric study of water vapor absorption into a constrained thin film of lithium bromide solution. *Int J Heat Mass Transf* 2012;55:5687–95.
- [4] Isfahani RN, Sampath K, Moghaddam S. Nanofibrous membrane-based absorption refrigeration system. *Int J Refrig* 2013;36:2297–307.
- [5] Isfahani RN, Moghaddam S. Absorption characteristics of lithium bromide (LiBr) solution constrained by superhydrophobic nanofibrous structures. *Int J Heat Mass Transf* 2013;63:82–90.
- [6] Asfand F, Stiriba Y, Bourouis M. Impact of the solution channel thickness while investigating the effect of membrane characteristics and operating conditions on the performance of water-LiBr membrane-based absorbers. *Appl Therm Eng* 2016;108:866–77.
- [7] Asfand F, Stiriba Y, Bourouis M. CFD simulation to investigate heat and mass transfer processes in a membrane-based absorber for water-LiBr absorption cooling systems. *Energy* 2015;91:517–30.
- [8] Bigham S, Yu D, Chugh D, Moghaddam S. Moving beyond the limits of mass transport in liquid absorbent microfilms through the implementation of surface-induced vortices. *Energy* 2014;65:621–30.
- [9] Bourouis M, Vallès M, Medrano M, Coronas A. Absorption of water vapour in the falling film of water-(LiBr + LiI + LiNO<sub>3</sub> + LiCl) in a vertical tube at air-cooling thermal conditions. *Int J Therm Sci* 2005;44:491–8.
- [10] Bourouis M, Vallès M, Medrano M, Coronas A. Performance of air-cooled absorption air conditioning systems working with water-(LiBr + LiI + LiNO<sub>3</sub> + LiCl). *J Process Mech Eng* 2005;219:205–12.
- [11] Medrano M, Bourouis M, Coronas A. Absorption of water vapour in the falling film of water-lithium bromide inside a vertical tube at air-cooling thermal conditions. *Int J Therm Sci* 2002;41:891–8.
- [12] Davidson W, Erickson D. 260 °C Aqueous absorption working pair under development. *News I EA Heat Pump Cent* 1986;4:29–31.
- [13] Howe L, Erickson D. Proof-of-Concept testing of alkali. Phase III. Final Report. USA: Energy Concepts Co.; 1990.
- [14] Erickson D, Potnis SV, Tang J. Triple effect absorption cycles. In: Energy conversion engineering conference IECEC 96. Proceedings of the 31st Intersociety; 1996. p. 1072–7.
- [15] Álvarez M, Esteve X, Bourouis M. Performance analysis of a triple-effect absorption cooling cycle using aqueous (lithium, potassium, sodium) nitrate solution as a working pair. *Appl Therm Eng* 2015;79:27–36.
- [16] Uemura T, Hasaba S. Studies on the lithium bromide-water absorption refrigeration machine, vol. 6. Technology Reports of Kansai University; 1964. p. 31–55.
- [17] Koo KK, Lee HR, Jeong S, Oh YS, Park DR, Baek YS. Solubilities, vapor pressures, and heat capacities of the water + lithium bromide + lithium nitrate + lithium iodide + lithium chloride system. *Int J Thermophys* 1999;20:589–600.
- [18] CREVER-URV. Thermophysical properties of the fluid mixture water/(LiBr + LiI + LiNO<sub>3</sub> + LiCl). Confidential Report. Spain: Universitat Rovira i Virgili; 2012.
- [19] Álvarez M, Bourouis M, Esteve X. Vapor-liquid equilibrium of aqueous alkaline nitrate and nitrite solutions for absorption refrigeration cycles with high temperature driving heat. *J Chem Eng Data* 2011;56:491–6.
- [20] Lee RJ, DiGiulio RM, Jeter SM, Teja AS. Properties of lithium bromide-water solutions at high temperatures and concentrations - II Density and viscosity. *ASHRAE Trans* 1990;709–14. Paper 3381. RP-527.
- [21] Álvarez ME. Theoretical and experimental study of the aqueous solution of lithium, sodium and potassium nitrates as a working fluid in absorption chillers driven by high temperature heat sources. PhD Thesis. Spain: Universitat Rovira i Virgili; 2013.
- [22] Kaita Y. Thermodynamic properties of lithium bromide–water solutions at high temperatures. *Int J Refrig* 2001;24:374–90.
- [23] Salavera D, Esteve X, Patil KR, Mainar AM, Coronas A. Solubility, heat capacity, and density of lithium bromide+lithium iodide+lithium nitrate+lithium chloride aqueous solutions at several compositions and temperature. *J Chem Eng Data* 2004;49:613–9.
- [24] Laliberté M. A model for calculating the heat capacity of aqueous solutions, with updated density and viscosity data. *J Chem Eng Data* 2009;54:1725–60.
- [25] DiGiulio RM, Lee RJ, Jeter SM, Teja AS. Properties of lithium bromide-water solutions at high temperatures and concentrations - I Thermal conductivity. *ASHRAE Trans* 1990;702–8. Paper 3380. RP-527.
- [26] Aseyev G. Electrolytes - properties of solutions methods for calculation of multicomponent systems, and experimental data on thermal conductivity and surface tension. New York: Begell House Publishers; 1998.
- [27] Florides GA, Kalogirou SA, Tassou SA, Wrobel LC. Design and construction of a LiBr–water absorption machine. *Energy Convers Manag* 2003;44:2483–508.
- [28] Asfand F, Bourouis M. Estimation of differential heat of dilution for aqueous lithium (bromide, iodide, nitrate, chloride) solution and aqueous (lithium, potassium, sodium) nitrate solution used in absorption cooling systems. *Int J Refrig* 2016. <http://dx.doi.org/10.1016/j.ijrefrig.2016.08.008>.
- [29] Ally M. Thermodynamic properties of aqueous ternary solutions relevant to chemical heat pumps. Final Report. ORNL/TM-10258. Oak Ridge National Laboratory; 1987.
- [30] Gierow M, Jernqvist A. Measurement of mass diffusivity with holographic interferometry for H<sub>2</sub>O/NaOH and H<sub>2</sub>O/LiBr working pairs. *Int Abs Heat Pump Conf* 1993;31:525–32.
- [31] Bird R, Stewart W, Lightfoot E. Transport phenomena. second ed. OUP; 2001.
- [32] Martínez L, Rodríguez-Maroto JM. On transport resistances in direct contact membrane distillation. *J Membr Sci* 2007;295:28–39.
- [33] ANSYS FLUENT UDF manual. ANSYS Inc.; November 2011. Release 14.0.
- [34] ANSYS FLUENT theory guide. ANSYS Inc.; November 2011. Release 14.0.